Accepted Manuscript

Synthesis and biological evaluation of bifendate derivatives bearing 6,7-dihydro-dibenzo[*c,e*]azepine scaffold as potential P-glycoprotein and tumor metastasis inhibitors

Xiaoke Gu, Yanfei Jiang, Yingying Qu, Jing Chen, Dingding Feng, Chenglin Li, Xiaoxing Yin

PII: S0223-5234(18)30019-9

DOI: 10.1016/j.ejmech.2018.01.019

Reference: EJMECH 10096

To appear in: *European Journal of Medicinal Chemistry*

Received Date: 23 October 2017

Revised Date: 28 December 2017

Accepted Date: 5 January 2018

Please cite this article as: X. Gu, Y. Jiang, Y. Qu, J. Chen, D. Feng, C. Li, X. Yin, Synthesis and biological evaluation of bifendate derivatives bearing 6,7-dihydro-dibenzo[*c,e*]azepine scaffold as potential P-glycoprotein and tumor metastasis inhibitors, *European Journal of Medicinal Chemistry* (2018), doi: 10.1016/j.ejmech.2018.01.019.

Synthesis and biological evaluation of bifendate derivatives bearing 6,7-dihydro-dibenzo[*c*,*e*]azepine scaffold as potential P-glycoprotein and tumor metastasis inhibitors

Xiaoke Gu[a, 1], Yanfei Jiang[a, 1], Yingying Qu[a], Jing Chen[a], Dingding Feng[a], Chenglin Li[a, *], Xiaoxing Yin[a, *]

[a]*Jiangsu Key Laboratory of New Drug Research and Clinical Pharmacy, Jiangsu Center for the Collaboration and Innovation of Cancer Biotherapy, Xuzhou Medical University, Xuzhou 221004, People's Republic of China*

Graphical Abstract

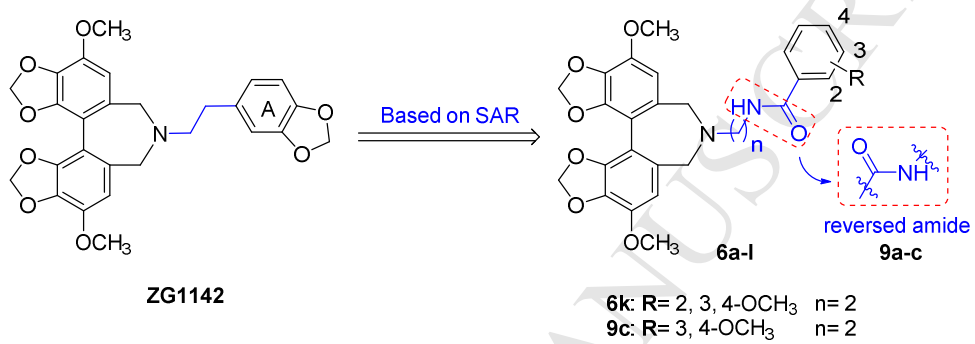

Compounds **6k** and **9c** exhibited significantly anti-MDR and anti-metastasis activities.

* Corresponding authors. Tel.: +86-516-83372005; fax: +86-516-83372005; e-mail: yinxx@xzhmu.edu.cn (X. Y.)
Tel.: +86-516-83262009; fax: +86-516-83262630; e-mail: licl@xzhmu.edu.cn (C. L.)
[1] These two authors contributed equally to this work.

Synthesis and biological evaluation of bifendate derivatives bearing 6,7-dihydro-dibenzo[*c,e*]azepine scaffold as potential P-glycoprotein and tumor metastasis inhibitors

Xiaoke Gu[a, 1], Yanfei Jiang[a, 1], Yingying Qu[a], Jing Chen[a], Dingding Feng[a], Chenglin Li[a, *], Xiaoxing Yin[a, *]

[a]*Jiangsu Key Laboratory of New Drug Research and Clinical Pharmacy, Jiangsu Center for the Collaboration and Innovation of Cancer Biotherapy, Xuzhou Medical University, Xuzhou 221004, People's Republic of China*

Abstract

As a continuation of previous research, fifteen bifendate derivatives bearing 6,7-dihydro-dibenzo [c,e]azepine scaffold were synthesized and evaluated as P-gp-medicated multidrug resistance (MDR) reversal agents. Biological evaluation indicated that compounds **6k** and **9c** more potently reversed P-gp-mediated MDR than bifendate and verapamil (VRP) by blocking P-gp mediated drug efflux function and not by decreasing P-gp expression in K562/A02 MDR cells. Interestingly, wound-healing and chamber migration assay showed that **6k** and **9c** could significantly attenuate the migration of MDA-MB-231 cells. Notably, **6k** and **9c** could markedly suppress the invasive activity of MDA-MB-231 cells, thus displayed potential anti-metastasis activity. Preliminary mechanism studies indicated that the anti-metastasis activity of **6k** and **9c** was associated with their inhibitory effect on the activity and expression of MMP-2 and MMP-9. These results, together with the MDR reversal results indicated that compounds **6k** and **9c** might be promising leads for developing novel anti-cancer agents with P-gp and tumor metastasis inhibitory activities.

Keywords: bifendate; dibenzo[*c*,*e*]azepine; P-gp inhibitor; multidrug resistance; metastasis.

1. Introduction

Multidrug resistance (MDR) is regarded as the leading cause for the failure of chemotherapy in cancer patients [1-3]. A well-established mechanism underlying MDR phenotype is the overexpression of ATP binding cassette (ABC) transporter superfamily [4-6]. Among these ABC transporters, P-glycoprotein

* Corresponding authors. Tel.: +86-516-83372005; fax: +86-516-83372005; e-mail: yinxx@xzhmu.edu.cn (X. Y.)
Tel.: +86-516-83262009; fax: +86-516-83262630; e-mail: licl@xzhmu.edu.cn (C. L.)

[1] These two authors contributed equally to this work.

(P-gp) is the best known and most important mediator of MDR, which can efflux various chemotherapeutic drugs out of tumor cells, leading to the decrease of intracellular drug levels and consequent drug insensitivity. Development of P-gp inhibitors is considered as a suitable and attractive strategy to overcome P-gp-mediated MDR [7-10]. As for this aspect, considerable attempts have been made to exploit P-gp inhibitor during past decades. However, no drug has been approved in clinic due to the poor potency, inherent toxicity and/or adverse pharmacokinetic interaction with anticancer drugs. Therefore, there is a clear and urgent requirement for developing novel P-gp inhibitors with safety and effective profiles.

Currently, natural products and their derivatives have been identified as novel and effective P-gp inhibitors by virtue of their advantages, such as low toxicity, few unfavorable pharmacokinetic interactions, etc [11-13]. Bifendate, an analogue of schisandrin C, can reverse P-gp-mediated MDR in vitro and in vivo by inhibiting P-gp, and more importantly, there was little pharmacokinetic interaction issue between bifendate and co-administered drugs, at least adriamycin (ADR) [14, 15]. Recently, we have described a series of bifendate derivatives bearing dibenzo[*c*,*e*]azepine scaffold as novel P-gp inhibitors [16]. Among the synthesized compounds, ZG1142 (Fig. 1) more potently reversed P-gp-mediated MDR than bifendate and classical P-gp inhibitor verapamil (VRP) through blocking P-gp efflux function, and persisted long chemo-sensitizing effect. More importantly, ZG1142 showed no stimulation on the P-gp ATPase activity, indicating that it is not a substrate of P-gp [16]. Structure-activity (SAR) relationships showed that the third benzene ring (A) was important for the P-gp inhibitory effect, and the length of the linker between nitrogen atom and the third benzene could significantly affect the P-gp inhibitory effects [16]. Previously SAR summarized in literatures showed that potent P-gp inhibitors were characterized with two or three aromatic moieties, a linker containing a tertiary nitrogen atom, hydrogen-bond acceptors and/or donors[17-19]. With these in mind and considering that a variable alkylphenyl linker incorporating an amide moiety is benefit for the P-gp inhibitory activities [20-24], we designed a new series of molecules (**6a-l**, Fig. 1) where the alkyl moiety between nitrogen atom and the third benzene of previous series was substituted with alkyl linkers incorporating an amide bond. In additional, the presence of a reverse-amide-bond (i.e., from NHCO to CONH) in the molecule may significantly affect the bioactivity of the target compound [25, 26]. Toward this end, three compounds (**9a-c**, Fig. 1) with a reverse-amide-bond were prepared. Thus, fifteen

compounds were synthesized, and their ability to overcome P-gp-mediated MDR was subsequently assessed.

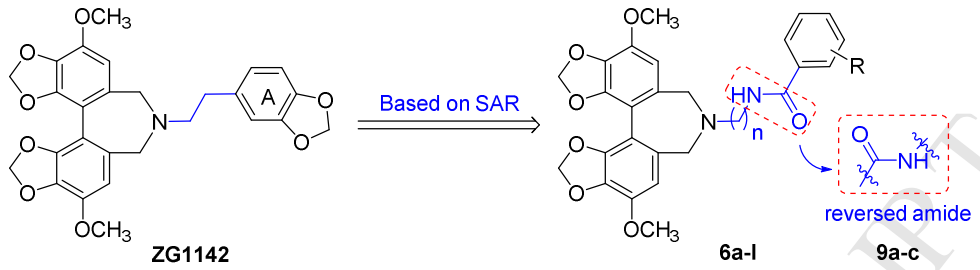

Figure 1. Chemical structure of ZG1142 and the target compounds (**6a-l**, **9a-c**)

2. Chemistry

The synthetic routes of the target compounds **6a-l** are depicted in Scheme 1. Compounds **2** and **3** were prepared starting from bifendate according to literature procedures [16]. Treatment of various diamines with Boc_2O afforded the mono-Boc-protected amines derivatives **1a-b**, which were directly reacted with **3** to produce the corresponding 6,7-dihydro-dibenzo[c,e]azepine intermediates **4a-b**, respectively. After the deletion of Boc group, compounds **5a-b** were subsequently condensed with various aromatic acids to produce the target compounds **6a-l**, respectively.

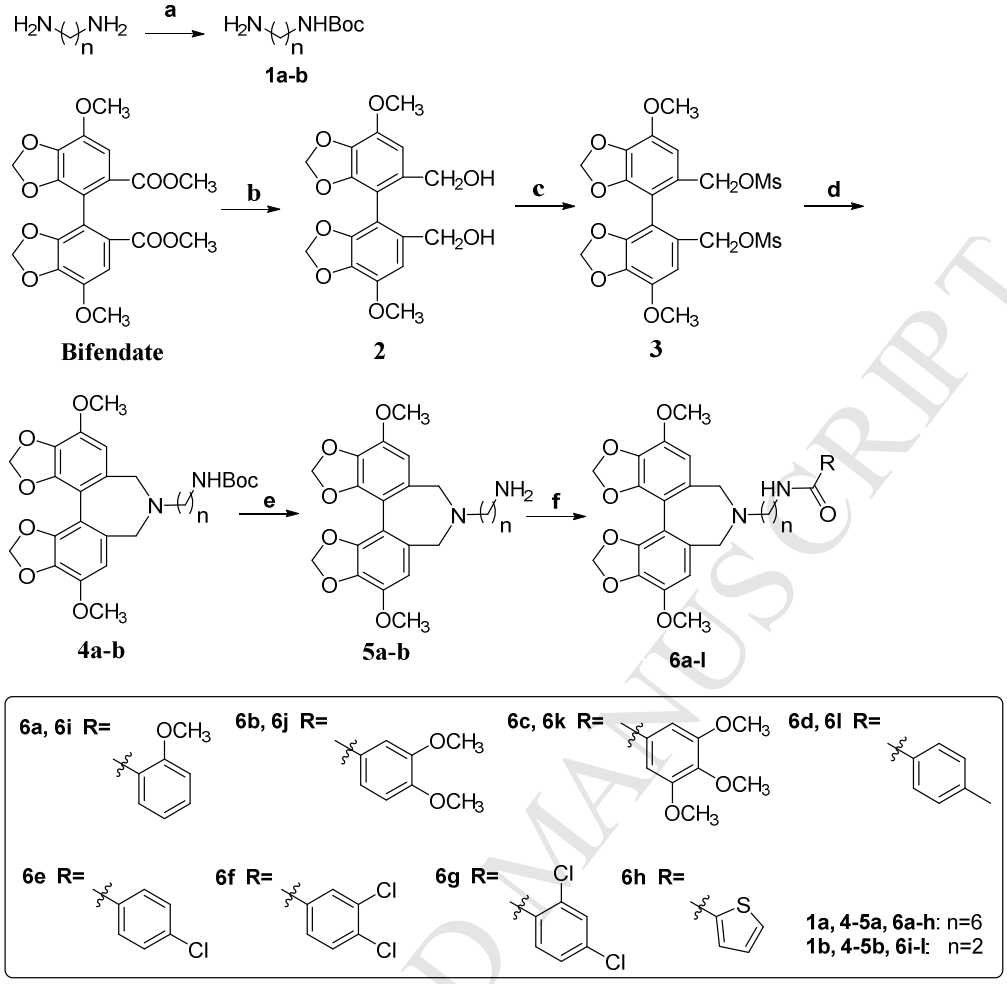

Scheme 1. Synthesis of the target compounds **6a-l**. Reagents and conditions: a) Boc_2O, $CHCl_3$, 0 °C-rt, 24 h; b) $LiAlH_4$, THF, 0 °C-rt, 4 h; c) methylsulfonyl chloride, Et_3N, CH_2Cl_2, rt, 6 h; d) **1a-b**, acetonitrile, Et_3N, 40 °C, 6-8 h; e) HCl/EtOH, 0 °C-rt, 12 h; f) RCOOH, HATU, Et_3N, DMF, rt, 6-8 h.

The synthetic routes of compounds **9a-c** are depicted in Scheme 2. Boc-β-Ala was condensed with various aromatic amines in the presence of HATU to afford the Boc-protected intermediates **7a-c**, respectively. After the deletion of Boc group, compounds **8a-b** were subsequently reacted with **3** to afford the target compounds **9a-c**, respectively.

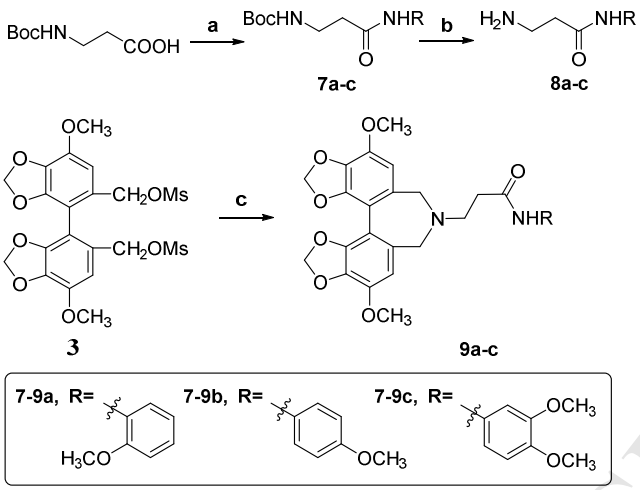

Scheme 2. Synthesis of the target compounds **9a-c**. Reagents and conditions: a) RNH_2, HATU, EtN_3, DMF, rt, 6-8 h; b) CF_3COOH, CH_2Cl_2, 0 °C-rt, 4-6 h; c) **8a-c**, acetonitrile, Et_3N, 40 °C, 6-8 h.

3. Results and discussion

3.1. Biological evaluation

3.1.1 Effect of the target compounds on Rh123 accumulation

It is well-known that P-gp transporter can efflux P-gp substrate chemotherapeutic drugs out of tumor cells, leading to the decrease of intracellular drug concentration and consequent drug insensitivity. Thus, flow cytometric analysis was firstly employed to assess the inhibitory effect of target compounds on P-gp by examining the intracellular accumulation of rhodamine 123 (Rh123, a P-gp fluorescent substrate) in P-gp-overexpressing K562/A02 cells. Classical P-gp inhibitor verapamil (VRP) was used as a positive control. As shown in Figure 2A, Rh123 level in K562/A02 cells treated with VRP was significantly increased, for the Rh123 accumulation fold change was 7.15. While, bifendate showed much weaker P-gp inhibitory effect than VRP, which is consistent with the previous report [15]. Interestingly, the target compounds, especially **6j**, **6k** and **9c**, significantly increased the intracellular Rh123 level in K562/A02 cells. Clearly, compound **9c** was the most potent one, and the value of Rh123 accumulation fold change was 9.32, which was even higher than that of positive control VRP and ZG1142.

Subsequently, the dose-response effects of the most active compounds **6j**, **6k**, **9c** and VRP (10, 3.3, 0.33 μM) on Rh123 accumulation in K562/A02 and parental sensitive K562 cells were further investigated by flow cytometry. As was expected, **6j**, **6k**, **9c** and VRP can significantly augment Rh123 accumulation in

K562/A02 cells at a dose-dependent manner, while this effect was not detected in P-gp-negative K562 cells (Fig. 2B), suggesting that such effect on Rh123 amassment in K562/A02 cells is likely achieved by inhibiting P-gp.

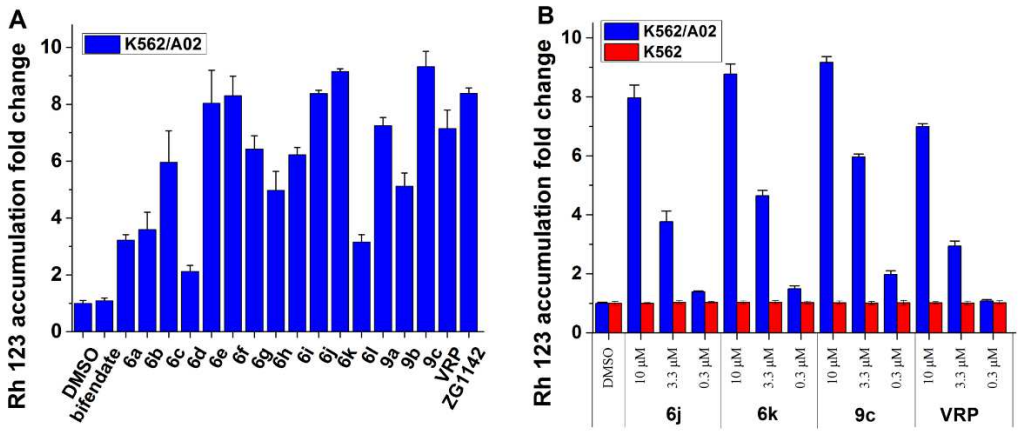

Figure 2. The effect of the target compounds (A: at the dose of 10 μM; B: at the dose of 10, 3.3 and 0.3 μM, respectively) on the intracellular accumulation of Rh123 (0.5 μM). The relative values were identified by dividing the fluorescence intensity of each measurement treated with compound or VRP by that of incubation with 0.1% DMSO. Data represents means ± S.D. of three independent experiments.

3.1.2 Cytotoxicity assays

Considering that a perfect P-gp inhibitor should overcome MDR at non-toxic doses [27, 28], we next determined the intrinsic cytotoxicity of the target compounds against K562/A02 (Table 1) and parental sensitive K562 cells (Table 2) by MTS assay using adriamycin (ADR) as the positive control. As was expected, K562/A02 cells overexpressing P-gp were insensitive to ADR (a substrate of P-gp), for the IC_{50} value of ADR for K562/A02 was 25.04 μM (Table 1), which was 64-fold higher than that for K562 cells (0.39 μM, Table 2). As shown in Table 1, most of the target compounds displayed slight intrinsic cytotoxicity (IC_{50} = 26.24 ~ 72.93 μM) against K562/A02 cells in *vitro*, and several compounds exhibited even higher cytotoxicity (IC_{50} = 11.47 ~ 23.31 μM). While, all the target compounds displayed relatively higher intrinsic cytotoxicity in K562 cells than that in K562/A02 cells (Table 2). Based on the IC_{50} values mentioned above, compounds at the concentration below IC_{10} were selected in the following MDR reversal experiments.

Table 1. IC_{50} values of target compounds against K562/A02 cells.

Compounds	IC_{50} (μM) [a]	Compounds	IC_{50} (μM) [a]	Compounds	IC_{50} (μM) [a]
6a	26.24 ± 0.53	**6g**	34.47 ± 1.18	**9a**	72.93 ± 3.42
6b	28.30 ± 1.99	**6h**	28.99 ± 0.89	**9b**	43.21 ± 3.12
6c	31.84 ± 0.86	**6i**	63.92 ± 1.32	**9c**	69.86 ± 2.90
6d	23.31 ± 2.23	**6j**	65.84 ± 3.21	**ADR**	25.04 ± 1.47
6e	18.36 ± 0.97	**6k**	47.22 ± 2.05	**ZG1142**	>100
6f	11.47 ± 0.05	**6l**	28.24 ± 0.63		

[a] IC_{50} values are expressed as means of triplicate experiments.

Table 2. IC_{50} values of target compounds against K562 cells.

Compounds	IC_{50} (μM) [a]	Compounds	IC_{50} (μM) [a]	Compounds	IC_{50} (μM) [a]
6a	10.96 ± 3.61	**6g**	13.67 ± 0.93	**9a**	23.05 ± 2.64
6b	14.11 ± 1.89	**6h**	12.54 ± 2.25	**9b**	29.82 ± 3.72
6c	11.82 ± 1.18	**6i**	15.03 ± 3.74	**9c**	34.78 ±1.37
6d	8.18 ± 1.16	**6j**	30.49 ± 1.74	**ADR**	0.39 ± 0.04
6e	5.85 ± 1.36	**6k**	16.87 ± 2.47	**ZG1142**	51.35 ± 0.42
6f	5.07 ± 1.18	**6l**	14.44 ±2.01		

[a] IC_{50} values are expressed as means of triplicate experiments.

*3.1.3 MDR reversal effects of **6k** and **9c***

To confirm whether compounds **6k** and **9c** can reverse P-gp mediated MDR, we next determined the cytotoxicity of ADR against K562/A02 cells in the presence or absence of the active compounds (**6k**, and **9c**) at non-toxic concentration (2.0 μM) by MTS assay, and VRP (2.0 μM) was selected as the positive control. Meanwhile, ZG1142, a potent P-gp inhibitor of bifendate derivative reported by us [16], was also selected as a positive control. As summarized in Table 3, IC_{50} value of ADR against K562/A02 was 24.44 μM, indicating that ADR alone exhibited poor inhibitory effect on the survival of K562/A02 cells. Interestingly, when ADR was combined with compounds **6k**, **9c** and VRP, the IC_{50} values of ADR was decreased to 6.40, 4.24 and 13.45 μM, respectively, indicating that all the compounds could sensitize K562/A02 cells to ADR at different levels. Clearly, **9c** displayed the most potent chemo-sensitizing effect.

The reversal fold (RF) of **9c** was 5.76, which was significantly higher than that of positive control VRP (RF = 1.82) and ZG1142 (RF = 3.99) at the same dose.

Table 3. Chemo-sensitizing effect of the target compounds

Compound	IC_{50} (μM) [a]	RF [b]	Compound	IC_{50} (μM) [a]	RF [b]
6k + ADR	6.40 ± 0.60	3.82	**VRP + ADR**	13.45 ± 0.87	1.82
9c + ADR	4.24 ± 0.29	5.76	**ADR**	24.44 ± 1.76	/
ZG1142 + ADR	6.13 ± 1.04	3.99			

[a] The cytotoxicity of ADR against K562/A02 cells in the presence or absence of the target compounds (2.0 μM) was evaluated by MTS assay.

[b] RF: Reversal fold (RF) refers to fold-change in drug sensitivity. RF = (IC_{50} of ADR without target compound)/(IC_{50} of ADR with target compound)

*3.1.4 Effect of active compounds **6k** and **9c** on P-gp expression and function*

It is believed that P-gp-mediated MDR can be overcame either by reducing P-gp expression and/or inhibiting its function [29]. To understand the potential molecular mechanisms underlying the action of **6k** and **9c**, we firstly tested the effect of **6k** and **9c** on P-gp expression at mRNA and protein levels using RT-PCR and Western blot, respectively. Data showed that treatment with **6k** and **9c** did not significantly change P-gp expression at mRNA or protein level in K562/A02 cells (shown in the Supplementary Material). These data suggested that compounds **6k** and **9c** may exert P-gp-mediated MDR reversal activity by inhibiting P-gp efflux function and not by decreasing P-gp expression.

*3.1.5 Anti-migratory and anti-invasive activities of **6k** and **9c***

Besides MDR, migration and invasion are also major causes of mortality in patients with cancer [30, 31]. Recent research showed that Schisandrin B (structure was shown in the Supplementary Material), a natural product with alkoxyl biphenyl scaffold, could attenuate cancer invasion and metastasis via inhibiting epithelial-mesenchymal transition [32]. In addition, in early studies, sun et al. found that bifendate could suppress the invasion of tumor cells [33]. With these in mind and considering that active compounds **6k** and **9c** shared the similar alkoxyl biphenyl scaffold as bifendate, we examined whether compounds **6k** and

9c could inhibit the migration and invasion of tumor cells. Due to the highly metastatic and invasive capacity, MDA-MB-231 cells (human breast carcinoma cells), were selected as models in this study.

Firstly, the effects of compounds **6k** and **9c** on the motility properties of MDA-MB-231 cells were determined by wound-healing assay and chamber migration assay, respectively [34]. As shown in Figure 3, at doses below IC_{50} (IC_{50} values of **6k** and **9c** were shown in the Supplementary Material), **6k** and **9c** significantly suppressed the migration of MDA-MB-231 cells across the wounded space in a dose depended manner. The inhibitory effect on cell mobility was subsequently confirmed by the chamber migration assay (Fig. 4). Exposure to **6k** and **9c** led to an obviously delay in cell migration up to 65.7% and 54.8%, respectively.

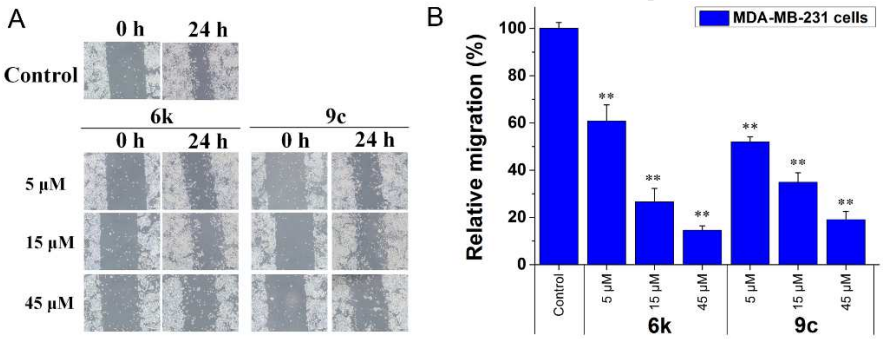

Figure 3. Inhibitory Effects of **6k** and **9c** on MDA-MB-231 cells migration *in vitro*. (A) Compounds inhibit migration of cells across the wounded space. Cell monolayer was wounded by a 200 μL pipette tip followed by treatment with various concentrations (5, 15, and 45 μM) of compound for 24 h. And distance of the wound edge was measured before and after the treatment. Image magnification: × 100. (B) Quantification of the relative migration. Relative migration (%) were identified by dividing the migration distance of MDA-MB-231 cells treated with **6k** or **9c** by that of control group. $^{**}P < 0.01$ represents significant difference from the control group.

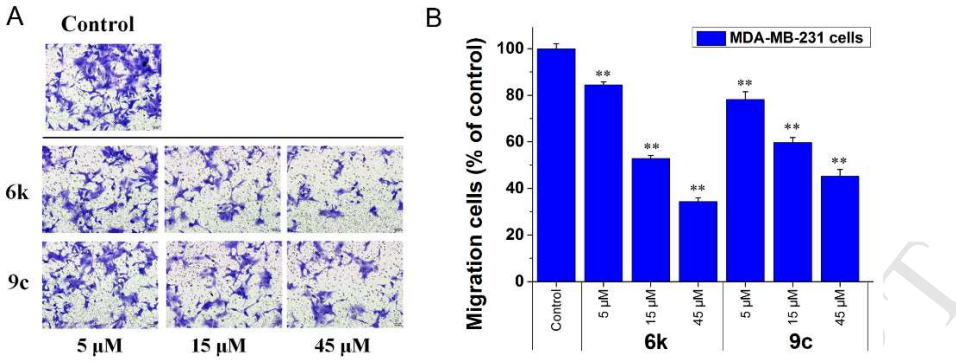

Figure 4. Effects of **6k** and **9c** on the mobility of MDA-MB-231 cells *in vitro*. (A) **6k** and **9c** inhibit cell migration. Cells were cultured with indicated concentrations of compounds for 24 h, and then seeded in the upside of transwell. After incubation for 4 h, the downward side of the membrane was stained with crystal violet. Image magnification: × 200. (B) Quantification of the migrated cells. Migration cells (% of control) were identified by dividing the number of the migration MDA-MB-231 cells treated with **6k** or **9c** by that of control group. $^{**}P < 0.01$ represents significant difference from the control group.

Next, the anti-invasive activities of **6k** and **9c** were determined by invasion assay. In the absence of compound **6k** or **9c**, most MDA-MB-231 cells were able to penetrate through the matrigel-coated filters, indicating its high invasive capability. After exposure to **6k** or **9c**, the number of MDA-MB-231 cells able to penetrate through the matrigel-coated filters was significantly decreased (Fig. 5), suggesting the invasive activity of MDA-MB-231 cells was markedly suppressed.

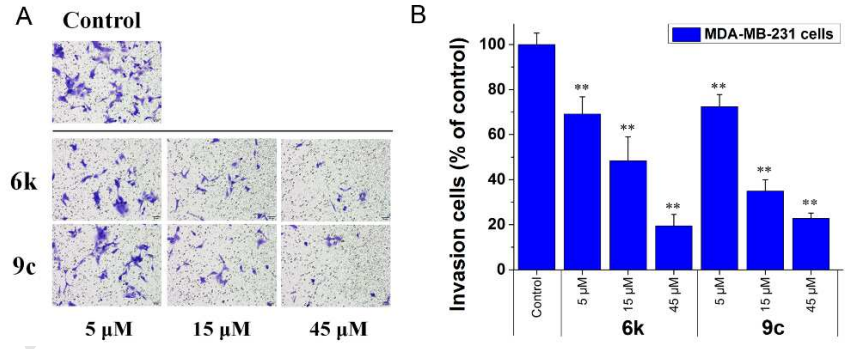

Figure 5. Effects of **6k** and **9c** on the invasion of MDA-MB-231 cells in vitro. (A) **6k** and **9c** inhibit cell invasion. After treatment with different concentrations of **6k** and **9c** for 24 h, the cells were seeded in the upside of transwell pre-coated with matrigel, and incubated for 24 h. Then, the invaded cells were measured by crystal violet staining. Image magnification: × 200. (B) Quantification of the invaded cells.

Invasion cells (% of control) were identified by dividing the number of the invasion MDA-MB-231 cells treated with **6k** or **9c** by that of control group. $^{**}P < 0.01$ represents significant difference from the control group.

*3.1.6 Effect of **6k** and **9c** on the activity and protein expression of MMP-2 and MMP-9*

It is well-known that matrix metalloproteinases (MMPs), especially MMP-2 and MMP-9, play critical roles in invasion and metastasis of malignant cells [35]. To probe the potential anti-invasive mechanisms, the effects of **6k** and **9c** on the activity and protein expression of MMP-2 and MMP-9 in MDA-MB-231 cells were determined by gelatin zymography assay and western blot, respectively. As shown in Figure 6, **6k** and **9c** significantly decreased the gelatinolytic activity of MMP-2 and MMP-9 in a dose dependent manner (Fig. 6A). Quantification analysis showed that treatment with **6k** or **9c**, even at the lowest concentration (5 μM), reduced MMP-2 activity to 59.1% and 52.8%, respectively, and MMP-9 activity was decreased to 58.2% and 52.6%, respectively. In addition, **6k** and **9c** could significantly suppress the protein expression of MMP-2 and MMP-9 in a dose dependent manner (Fig. 6B). These data suggested that the anti-metastatic activity of **6k** and **9c** was associated with their inhibitory effect on MMP-2 and MMP-9 activity and expression.

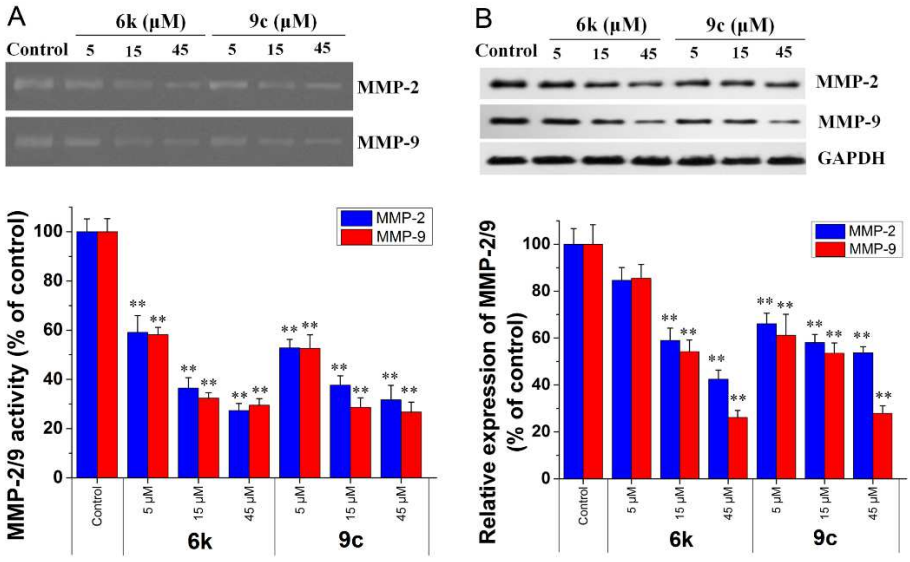

Figure 6. Effects of **6k** and **9c** on the activity and expression of MMP-2 and MMP-9 in MDA-MB-231 cells. (A) **6k** and **9c** inhibit the activity of MMP-2/9 in MDA-MB-231 cells. Cells were treated with indicated concentrations of **6k** and **9c** for 24 h. The culture supernatants were collected, and then MMP-2/9

activity was determined by gelatin zymography assay. (B) **6k** and **9c** suppress the protein expression of MMP-2/9. MDA-MB-231 cell lysates were subjected to immunoblotting with antibodies against MMP-2 and MMP-9. $^{**}P < 0.01$ represents significant difference from the control group.

3.2. Structure-Activity Relationships

Based on the results above, structure-activity relationships (SARs) of the target compounds on P-gp inhibitory effects could be summarized as follows: The length of the linker between the benzene ring and nitrogen atom in azepine ring can significantly affect P-gp inhibitory effect. Compounds with a four atoms chain displayed higher inhibitory effect on P-gp than that with an eight atoms chain (**6i** *vs*. **6a**, **6j** *vs*. **6b**, **6k** *vs*. **6c**, **6l** *vs*. **6d**). Interestingly, introducing methoxyl substitutes to the third benzene ring could significantly increase the intensity of P-gp inhibition (**6k** *vs.* **6j** *vs.* **6i**, **6c** *vs.* **6b** *vs.* **6a**). P-gp inhibitory effect can enhanced by changing methoxy or methyl into chlorine atom in the third benzene ring, unfortunately, the intrinsic cytotoxicity was also increased (**6b** *vs.* **6f**, **6d** *vs*. **6e**). Notably, when amide-bond was reversed (from NHCO to CONH) in the molecule, the P-gp inhibitory intensity was significantly increased (**9a** *vs.* **6i**, **9c** *vs.* **6j**), which was consistent with previously reported that a reverse-amide-bond can significantly affect the bioactivity of the target compounds. One plausible explanation is that reverse of amide might affect the affinity between target compounds with P-gp, and consequent weak P-gp inhibitory intensity. However, the precise SARs remain further investigation when more derivatives of this kind will be available in near future.

4. Conclusions

In summary, fifteen novel bifendate derivatives containing dibenzo[*c*,*e*]azepine scaffold were synthesized and evaluated as P-gp-medicated MDR reversal agents. Among them, compounds **6k** and **9c** more potently increased the accumulation of P-gp substrate in K562/A02 cells than VRP by inhibiting P-gp efflux function instead by decreasing P-gp protein expression levels. Notably, wound-healing and chamber migration assay showed that **6k** and **9c** could significantly attenuate the motility of MDA-MB-231 cells. More importantly, **6k** and **9c** could markedly suppress the invasive activity of MDA-MB-231 cells, thus displayed potential anti-metastasis activity. Preliminary mechanism studies indicated that the

anti-metastasis activity of **6k** and **9c** were associated with their inhibitory effect on MMP-2 and MMP-9 activity and expression. These results, together with the MDR reversal results suggested that compounds **6k** and **9c** might be promising leads for the development novel anti-cancer agents with P-gp and tumor metastasis inhibitory activities.

5. Experimental protocols

5.1. Chemical analysis

All of the synthesized compounds were purified by column chromatography on silica gel 60 (200–300 mesh) or thin layer chromatography (TLC) on silica gel 60 F254 plates (250 mm; Qingdao Ocean Chemical Company, China). Melting points were measured on a YRT-3 melting point apparatus and uncorrected. Subsequently, all of them were analyzed by IR (Thermofisher Nicolet is10), ^{1}HNMR and ^{13}C NMR (JEOL, 400 MHz), and MS (Agilent 1290/6460 LC/MSD spectrometer) routinely. All solvents were reagent grade and, when necessary, were purified and dried by standards methods.

*5.2. Synthesis of **1a-b***

Ethane diamine (6 g, 0.1 mol) or hexamethylenediamine (12 g, 0.1 mol) was dissolved in $CHCl_3$ (100 mL) and cooled to 0 °C. Boc_2O (4.6 mL, 0.01 mol) was dispersed in $CHCl_3$ (100 mL) and the mixture was added to the above reaction solution slowly. Then, the solution was stirred for 24 h at room temperature. After the completion of reaction, the mixture was evaporated in vacuo and the residue was diluted with water and extracted with $CHCl_3$. The organic layer was washed sequentially with saturated $NaHCO_3$ solution and brine then dried with sodium sulfate, filtered and evaporated in vacuo to give corresponding crude compounds **1a-b** (92%), respectivley, which were used without further purification.

*5.3. Synthesis of **5a-b***

Et_3N (1.2 mL, 5eq) was added to the stirred solution of compound **3** and **1a** (2eq) in acetonitrile at room temperature under a nitrogen atmosphere. The reaction mixture was stirred and refluxed for 5 h at 60 °C. After the completion of reaction, the mixture was evaporated in vacuo and the residue was diluted with water and extracted with ethyl acetate. The organic layer was washed sequentially with saturated $NaHCO_3$

solution and brine, then dried with sodium sulfate, filtered and evaporated in vacuo to give corresponding crude compound **4a**. And then the Boc-protection group is removed using hydrochloric acid in ethanol to afford compound **5a**, which was used without further purification. The title crude compound **5b** was obtained starting from **3** and **1a**.

*5.4. General procedure for the preparation of **6a-l***

A solution of **5a** or **5b**, triethylamine and substituted benzoic acid in DMF was stirred at 0 °C, then HATU was added to the solution. The reaction mixture was stirred at 0 °C for 1 h, then diluted with saturated aqueous $NaHCO_3$ and extracted with EtOAc. The organic layer was washed with brine, dried with anhydrous sodium sulfate, filtered and evaporated in vacuum. The crude product was purified by column chromatography to yield the title compounds, respectively.

5.4.1.N-(6-(4,10-dimethoxy-6H-[1,3]dioxolo[4',5':3,4]benzo[1,2-c][1,3]dioxolo[4',5':5,6]benzo[1,2-e]azepin-7(8H)-yl)hexyl)-2-methoxybenzamide **(6a)**

The title compound was obtained starting from **5a** and 2-methoxybenzoic acid. As a yellow solid, yield: 64.2%; mp: 129.8-131.6 °C. Analytical data for **6a**: ^{1}H NMR ($CDCl_3$, 400 MHz, δ ppm): 1.42-1.59 (m, 4H), 1.60-1.72 (m, 2H), 1.85-2.00 (m, 2H), 3.03-3.33 (m, 2H), 3.39-3.52 (m, 2H), 3.93 (s, 6H, 2 × Ar-OCH_3), 3.98 (s, 3H, Ar-OCH_3), 4.09-4.24 (m, 2H), 6.05 (d, 2H, -OCH_2O-, *J* = 1.4 Hz), 6.14 (d, 2H, -OCH_2O-, *J* = 1.4 Hz), 6.85 (s, 2H, 2 × Ar-H), 6.95-7.01 (m, 2H, 2 × Ar-H), 7.43 (m, 1H, Ar-H), 7.91-7.93 (m, 1H, Ar-H), 8.08 (t, 1H, -NH-, *J* = 5.7 Hz); ^{13}C NMR ($CDCl_3$, 100 MHz, δ ppm): 24.7, 25.8, 26.0, 29.1, 39.5, 54.3，54.4, 56.1 (2C, 2 × $ArCH_2N$), 57.0 (2C, 2 × OCH_3), 102.5 (2C, 2 × -OCH_2O-), 110.2, 111.4, 111.6 (2C, 2 × Ar-C), 121.1, 121.2 (2C, 2 × Ar-C), 131.7 (2C, 2 × Ar-C), 133.2 (2C, 2 × Ar-C), 137.0 (2C, 2 × Ar-C), 143.8 (2C, 2 × Ar-C), 146.4 (2C, 2 × Ar-C), 157.7, 166.0 (-CONH-); IR (KBr, cm^{-1}): ν 3398, 2943, 2360, 1644, 1600, 1544, 1496, 1439, 1384, 1311, 1148, 1102, 1058, 923, 841; ESI-MS: m/z: 577.2 $[M+H]^+$.

5.4.2.N-(6-(4,10-dimethoxy-6H-[1,3]dioxolo[4',5':3,4]benzo[1,2-c][1,3]dioxolo[4',5':5,6]benzo[1,2-e]azepin-7(8H)-yl)hexyl)-3,4-dimethoxybenzamide **(6b)**

The title compound was obtained starting from **5a** and 3,4-dimethoxybenzoic acid. As a yellow solid, yield: 60.4%; mp: 129.8-131.6 °C. Analytical data for **6b**: ^{1}H NMR ($CDCl_3$, 400 MHz, δ ppm): 1.39-1.49 (m, 4H), 1.57-1.68 (m, 2H), 1.70-1.90 (m, 2H), 2.86-3.11 (m, 2H), 3.36-3.54 (m, 4H), 3.87 (s, 3H, OCH_3), 3.88 (s, 3H, OCH_3), 3.91 (s, 6H, 2 × -OCH_3), 3.97 (s, 1H), 4.00 (s, 1H), 6.02 (d, 2H, -OCH_2O-, *J* = 1.2 Hz), 6.12 (d, 2H, Ar-OCH_2O-, *J* = 1.2 Hz), 6.74 (s, 2H, Ar-H), 6.83 (d, 1H, Ar-H, *J* = 8.0 Hz), 7.29-7.35 (m, 2H, Ar-H); ^{13}C NMR ($CDCl_3$, 100 MHz, δ ppm): 26.7, 26.9, 27.0, 29.5, 40.0, 54.8, 54.9 (2C, 2 × OCH_3), 56.1 (2C, 2 × $ArCH_2N$), 56.9 (2C, 2 × OCH_3), 102.0 (2C, 2 × -OCH_2O-), 109.7 (2C, 2 × Ar-C), 110.3, 110.5, 110.6 (2C, 2 × Ar-C), 119.3 (2C, 2 × Ar-C), 127.4 (2C, 2 × Ar-C), 135.4 (2C, 2 × Ar-C), 143.1 (2C, 2 × Ar-C), 145.9 (2C, 2 × Ar-C), 149.0, 151.7, 167.3 (-CONH-); IR (KBr, cm^{-1}): ν 3413,2939, 2360, 2341, 1639, 1617, 1582, 1507, 1437, 1311, 1230, 1147, 1101, 1048, 922, 844; ESI-MS: m/z: 607.2 $[M+H]^+$.

5.4.3.N-(6-(4,10-dimethoxy-6H-[1,3]dioxolo[4',5':3,4]benzo[1,2-c][1,3]dioxolo[4',5':5,6]benzo[1,2-e]azepin-7(8H)-yl)hexyl)-3,4,5-trimethoxybenzamide **(6c)**

The title compound was obtained starting from **5a** and 3,4,5-trimethoxybenzoic acid. As a yellow solid, yield: 61.6%; mp: 134.2-136.1 °C. Analytical data for **6c**: ^{1}H NMR ($CDCl_3$, 400 MHz, δ ppm): 1.35-1.50 (m, 4H), 1.55-1.69 (m, 2H), 1.71-1.98 (m, 2H), 2.17-2.37 (m, 1H), 3.00-3.13 (m, 1H), 3.20-3.48 (m, 4H), 3.81-3.86 (m, 12H, 4 × Ar -OCH_3), 3.97 (s, 3H, Ar-OCH_3), 4.00-4.05 (m, 1H), 4.29-4.33 (m, 1H), 6.04 (dd, 2H, -OCH_2O-, *J* = 6.4, 1.2 Hz), 6.13 (dd, 2H, -OCH_2O-, *J* = 9.2, 1.2 Hz), 6.81 (d, 2H, 2 × Ar-H, *J* = 4.4 Hz), 7.01 (s, 2H, 2 × Ar-H), 8.75 (s, 1H, -NH-); ^{13}C NMR ($CDCl_3$, 100 MHz, δ ppm): 24.2, 25.6, 25.7, 28.5, 40.3, 53.5, 54.3, 54.9, 56.3 (2C, 2 × $ArCH_2N$), 56.7, 57.2, 61.0, 102.5 (2C, 2 × -OCH_2O-), 104.5 (2C, 2 × Ar-C), 110.0, 110.3, 111.2, 111.8, 120.0, 122.4, 129.0, 137.1, 137.3, 140.9, 143.7, 143.9, 146.3, 146.6, 153.2 (2C, 2 × Ar-C), 168.4 (-CONH-); IR (KBr, cm^{-1}): ν 3414, 2942, 2360, 2341, 1643, 1617, 1584, 1499, 1437, 1383, 1311, 1235, 1148, 1102, 1058, 922, 844; ESI-MS: m/z: 637.2 $[M+H]^+$.

5.4.4.N-(6-(4,10-dimethoxy-6H-[1,3]dioxolo[4',5':3,4]benzo[1,2-c][1,3]dioxolo[4',5':5,6]benzo[1,2-e]azepin-7(8H)-yl)hexyl)-4-methylbenzamide **(6d)**

The title compound was obtained starting from **5a** and 4-methylbenzoic acid. As a yellow solid, yield: 50.2%; mp: 101.6-103.2 °C. Analytical data for **6d**: ^{1}H NMR ($CDCl_3$, 400 MHz, δ ppm): 1.36-1.48 (m, 4H),

1.56-1.62 (m, 4H), 2.37 (s, 3H, -CH_3), 2.44-2.66 (m, 2H), 3.20 (d, 2H, *J* = 12.4 Hz), 3.41-3.46 (m, 2H), 3.57 (d, 2H, *J* = 12.8 Hz), 3.92 (s, 6H, 2 × Ar-OCH_3), 5.97 (d, 2H, -OCH_2O-, *J* = 1.2 Hz), 6.08 (d, 2H, -OCH_2O-, *J* = 1.2 Hz), 6.56 (s, 2H, 2 × Ar-H), 7.20 (d, 2H, 2 × Ar-H, *J* = 8.0 Hz), 7.64 (d, 2H, 2 × Ar-H, *J* = 8 Hz); ^{13}C NMR ($CDCl_3$, 100 MHz, δ ppm): 21.5, 26.9, 27.2, 27.5, 29.66, 40.0, 55.0 (2C, 2 × ArCH_2N), 55.2, 56.8 (2C, 2 × OCH_3), 101.9 (2C, 2 × -OCH_2O-), 109.4 (2C, 2 × Ar-C), 110.6 (2C, 2 × Ar-C), 126.9 (2C, 2 × Ar-C), 128.4 (2C, 2 × Ar-C), 129.3 (2C, 2 × Ar-C), 131.9, 135.1 (2C, 2 × Ar-C), 141.9, 143.0 (2C, 2 × Ar-C), 145.8 (2C, 2 × Ar-C), 167.6 (-CONH-); IR (KBr, cm^{-1}): ν 3413, 2931, 2360, 2341, 1639, 1616, 1541, 1506, 1435, 1374, 1306, 1143, 1099, 1050, 925, 842; ESI-MS: m/z: 561.2 $[M+H]^+$.

5.4.5.4-chloro-N-(6-(4,10-dimethoxy-6H-[1,3]dioxolo[4',5':3,4]benzo[1,2-c][1,3]dioxolo[4',5':5,6]benzo[1,2-e]azepin-7(8H)-yl)hexyl)benzamide **(6e)**

The title compound was obtained starting from **5a** and 4-chlorobenzoic acid. As a yellow solid, yield: 52.3%; mp: 75.5-76.8 °C. Analytical data for **6e**: ^{1}H NMR ($CDCl_3$, 400 MHz, δ ppm): 1.39-1.45 (m, 4H), 1.59-1.76 (m, 4H), 2.50-2.74 (m, 2H), 3.28 (d, 2H, *J* = 12.5 Hz), 3.39-3.51 (m, 2H), 3.62 (d, 2H, *J* = 12.4 Hz), 3.93 (s, 6H, 2 × Ar-OCH_3), 5.99 (d, 2H, -OCH_2O-, *J* = 1.3 Hz), 6.09 (d, 2H, -OCH_2O-, *J* = 1.4 Hz), 6.59 (s, 2H, 2 × Ar-H), 7.36-7.41 (m, 2H, 2 × Ar-H), 7.70-7.76 (m, 2H, 2 × Ar-H); ^{13}C NMR ($CDCl_3$, 100 MHz, δ ppm): 26.6, 26.9, 27.0, 29.4, 40.0, 54.7 (3C, 3 × NCH_2), 56.9 (2C, 2 × OCH_3), 102.0 (2C, 2 × -OCH_2O-), 109.9 (2C, 2 × Ar-C), 110.5 (2C, 2 × Ar-C), 128.5 (2C, 2 × Ar-C), 128.9 (2C, 2 × Ar-C), 133.1 (2C, 2 × Ar-C), 135.4 (2C, 2 × Ar-C), 137.6, 137.7, 143.1 (2C, 2 × Ar-C), 145.9 (2C, 2 × Ar-C), 166.6 (-CONH-); IR (KBr, cm^{-1}): ν 3413, 2932, 2359, 2341, 1638, 1540, 1488, 1434, 1384, 1306, 1144, 1098, 1051, 925, 846; ESI-MS: m/z: 581.1 $[M+H]^+$.

5.4.6.3,4-dichloro-N-(6-(4,10-dimethoxy-6H-[1,3]dioxolo[4',5':3,4]benzo[1,2-c][1,3]dioxolo[4',5':5,6]benzo[1,2-e]azepin-7(8H)-yl)hexyl)benzamide **(6f)**

The title compound was obtained starting from **5a** and 3,4-dichlorobenzoic acid. As a yellow solid, yield: 53.4%; mp: 85.5-88.3 °C. Analytical data for **6f**: ^{1}H NMR ($CDCl_3$, 400 MHz, δ ppm): 1.40-1.53 (m, 4H), 1.62-1.74 (m, 2H), 1.77-1.97 (m, 2H), 2.77-2.96 (m, 2H), 3.41-3.52 (m, 4H), 3.88 (d, 2H, *J* = 12.8 Hz), 3.96 (s, 6H, 2 × Ar-OCH_3), 6.03 (d, 2H, -OCH_2O-, *J* = 1.2 Hz), 6.13 (d, 2H, -OCH_2O-, *J* = 1.2 Hz), 6.72 (s,

2H, 2 × Ar-H), 7.49 (d, 1H, Ar-H, *J* = 8.4 Hz), 7.755-7.78 (m, 1H, Ar-H), 8.04 (d, 1H, Ar-H, *J* = 2.0 Hz); ^{13}C NMR ($CDCl_3$, 100 MHz, δ ppm): 25.1, 25.9, 26.2, 28.8, 39.8, 53.7, 53.9 (2C, 2 × $ArCH_2N$), 57.1 (2C, 2 × OCH_3), 102.3 (2C, 2 × -OCH_2O-), 110.3 (2C, 2 × Ar-C), 111.0 (2C, 2 × Ar-C), 123.9, 126.6, 129.6 (2C, 2 × Ar-C), 130.5, 132.9, 134.5, 135.6, 136.4 (2C, 2 × Ar-C), 143.4 (2C, 2 × Ar-C), 146.3 (2C, 2 × Ar-C), 165.5 (-CONH-); IR (KBr, cm^{-1}): ν 3415, 2933, 2360, 2341, 1637, 1540, 1489, 1435, 1384, 1310, 1148, 1100, 1044, 923, 840; ESI-MS: m/z: 615.1 $[M+H]^+$.

5.4.7.2,4-dichloro-N-(6-(4,10-dimethoxy-6H-[1,3]dioxolo[4',5':3,4]benzo[1,2-c][1,3]dioxolo[4',5':5,6]benzo[1,2-e]azepin-7(8H)-yl)hexyl)benzamide **(6g)**

The title compound was obtained starting from **5a** and 2,4-dichlorobenzoic acid. As a yellow solid, yield: 49.0%; mp: 70.2-72.3 °C. Analytical data for **6g**: ^{1}H NMR ($CDCl_3$, 400 MHz, δ ppm): 1.39-1.52 (m, 4H), 1.61-1.67 (m, 2H), 1.82-1.98 (m, 2H), 2.86-3.01 (m, 2H), 3.41-3.46 (m, 4H), 3.90 (s, 6H, 2 × Ar-OCH_3), 4.00-4.08 (m, 2H), 6.01 (d, 2H, -OCH_2O-, *J* = 1.6 Hz), 6.11 (d, 2H, -OCH_2O-, *J* = 1.2 Hz), 6.68 (s, 2H, Ar-H), 7.13-7.18 (m, 1H, Ar-H), 7.38 (d, 1H, Ar-H, *J* = 2.0 Hz), 7.54 (s, 1H, Ar-H), 7.56 (s, 1H, Ar-H); ^{13}C NMR ($CDCl_3$, 100 MHz, δ ppm): 24.9, 26.0, 26.4, 28.8, 39.8, 53.3, 53.5 (2C, 2 × $ArCH_2N$), 57.0 (2C, 2 × OCH_3), 102.2 (2C, 2 × -OCH_2O-), 110.4 (2C, 2 × Ar-C), 111.0 (2C, 2 × Ar-C), 126.6, 127.5, 129.8, 130.0 (2C, 2 × Ar-C), 130.9, 131.1, 134.0, 136.4 (2C, 2 × Ar-C), 143.4 (2C, 2 × Ar-C), 146.3 (2C, 2 × Ar-C), 165.6 (-CONH-); IR (KBr, cm^{-1}): ν 3413, 2936, 2360, 1640, 1616, 1555, 1490, 1436, 1383, 1309, 1146, 1101, 1046, 923, 845; ESI-MS: m/z: 615.1 $[M+H]^+$.

5.4.8.N-(6-(4,10-dimethoxy-6H-[1,3]dioxolo[4',5':3,4]benzo[1,2-c][1,3]dioxolo[4',5':5,6]benzo[1,2-e]azepin-7(8H)-yl)hexyl)thiophene-2-carboxamide **(6h)**

The title compound was obtained starting from **5a** and thiophene-2-carboxylic acid. As a yellow solid, yield: 65.8%; mp: 84.7-86.4 °C. Analytical data for **6h**: ^{1}H NMR ($CDCl_3$, 400 MHz, δ ppm): 1.33-1.46 (m, 4H), 1.52-1.67 (m, 4H), 2.40-2.59 (m, 2H), 3.17 (d, 2H, *J* = 12.4 Hz), 3.42 (m, 2H), 3.51 (d, 2H, *J* = 12.4 Hz), 3.92 (s, 6H, 2 × Ar-OCH_3), 5.96 (d, 2H, -OCH_2O-, *J* = 1.4 Hz), 6.07 (d, 2H, -OCH_2O-, *J* = 1.4 Hz), 6.54 (s, 2H, 2 × Ar-H), 7.03-7.05 (m, 1H), 7.42-7.44 (m, 1H), 7.48-7.50 (m, 1H); ^{13}C NMR ($CDCl_3$, 100 MHz, δ ppm): 26.9, 27.3, 27.7, 29.7, 40.0, 55.0 (2C, 2 × $ArCH_2N$), 55.1, 56.8 (2C, 2 × OCH_3), 101.8 (2C, 2

× -OCH_2O-), 109.3 (2C, 2 × Ar-C), 110.7 (2C, 2 × Ar-C), 127.7, 127.9, 129.0, 129.8 (2C, 2 × Ar-C), 134.9 (2C, 2 × Ar-C), 139.3, 142.9 (2C, 2 × Ar-C), 145.8 (2C, 2 × Ar-C), 162.0 (-CONH-); IR (KBr, cm^{-1}): ν 3413, 2932, 2360, 2341, 1637, 1617, 1541, 1506, 1432, 1373, 1304, 1209, 1142, 1098, 1050, 924, 844; ESI-MS: m/z: 553.1 $[M+H]^+$.

5.4.9.N-(2-(4,10-dimethoxy-6H-[1,3]dioxolo[4',5':3,4]benzo[1,2-c][1,3]dioxolo[4',5':5,6]benzo[1,2-e]azepin-7(8H)-yl)ethyl)-2-methoxybenzamide **(6i)**

The title compound was obtained starting from **5b** and 2-methoxybenzoic acid. As a yellow solid, yield: 59.3%; mp: 74.9-76.3 °C. Analytical data for **6i**: ^1H NMR (DMSO, 400 MHz, δ ppm): 2.49-2.51 (m, 2H), 3.14-3.22 (m, 2H), 3.29-3.41 (m, 2H), 3.64-3.83 (m, 2H), 3.90 (s, 6H, 2 × Ar-OCH_3), 3.92 (s, 3H, Ar-OCH_3), 6.09 (d, 2H, -OCH_2O-, *J* = 0.8 Hz), 6.13 (d, 2H, -OCH_2O-, *J* = 0.8 Hz), 6.96-7.02 (m, 1H, Ar-H), 7.05-7.09 (m, 1H, Ar-H), 7.17-7.21 (m, 1H, Ar-H), 7.49-7.55 (m, 1H, Ar-H), 7.84-7.88 (m, 1H, Ar-H), 8.54-8.57 (m, 1H, Ar-H); ^{13}C NMR (DMSO, 100 MHz, δ ppm): 35.5, 38.8, 52.9, 56.5 (2C, 2 × $ArCH_2N$), 57.1 (2C, 2 × OCH_3), 102.7 (2C, 2 × -OCH_2O-), 110.6 (2C, 2 × Ar-C), 112.7 (2C, 2 × Ar-C), 121.1 (2C, 2 × Ar-C), 122.6, 131.2 (2C, 2 × Ar-C), 133.3 (2C, 2 × Ar-C), 136.7 (2C, 2 × Ar-C), 143.3 (2C, 2 × Ar-C), 146.5 (2C, 2 × Ar-C), 157.7, 166.3 (-CONH-); IR (KBr, cm^{-1}): ν 3412, 2908, 1643, 1619, 1545, 1496, 1444, 1396, 1312, 1243, 1172, 1107, 1047, 918, 839; ESI-MS: m/z: 521.2 $[M+H]^+$.

5.4.10.N-(2-(4,10-dimethoxy-6H-[1,3]dioxolo[4',5':3,4]benzo[1,2-c][1,3]dioxolo[4',5':5,6]benzo[1,2-e]azepin-7(8H)-yl)ethyl)-3,4-dimethoxybenzamide **(6j)**

The title compound was obtained starting from **5b** and 3,4-dimethoxybenzoic acid. As a yellow solid, yield: 56.1%; mp: 90.6-92.4 °C. Analytical data for **6j**: ^1H NMR ($CDCl_3$, 400 MHz, δ ppm): 2.64-2.96 (m, 2H), 3.27 (d, 2H, *J* = 12.4 Hz), 3.51-3.60 (m, 2H), 3.61-3.70 (m, 2H), 3.95 (s, 12H, 4 × Ar-OCH_3), 6.00 (s, 2H, -OCH_2O-), 6.10 (s, 2H, -OCH_2O-), 6.57 (s, 2H, 2 × Ar-H), 6.88 (d, 1H, Ar-H, *J* = 7.7 Hz), 7.01 (dd, 1H, Ar-H, *J* = 1.3, 0.8 Hz), 7.30-7.39 (m, 1H, Ar-H), 7.49 (s, 1H, Ar-H); ^{13}C NMR ($CDCl_3$, 100 MHz, δ ppm): 37.3, 53.8, 54.9 (2C, 2 × OCH_3), 56.1 (2C, 2 × $ArCH_2N$), 56.9 (2C, 2 × OCH_3), 101.9 (2C, 2 × -OCH_2O-), 109.3 (2C, 2 × Ar-C), 110.3, 110.7 (2C, 2 × Ar-C), 110.8, 119.5, 127.3, 128.6 (2C, 2 × Ar-C), 135.1 (2C, 2 × Ar-C), 143.0 (2C, 2 × Ar-C), 145.9 (2C, 2 × Ar-C), 149.0, 151.8, 167.3 (-CONH-); IR (KBr, cm^{-1}): ν

3413, 2937, 1639, 1604, 1584, 1544, 1506, 1433, 1383, 1305, 1229, 1182, 1097, 1047, 924, 856; ESI-MS: m/z: 551.2 $[M+H]^+$.

5.4.11.N-(2-(4,10-dimethoxy-6H-[1,3]dioxolo[4',5':3,4]benzo[1,2-c][1,3]dioxolo[4',5':5,6]benzo[1,2-e]azepin-7(8H)-yl)ethyl)-3,4,5-trimethoxybenzamide **(6k)**

The title compound was obtained starting from **5b** and 3,4,5-trimethoxybenzoic acid. As a yellow solid, yield: 53.2%; mp: 122.1-123.8 °C. Analytical data for **6k**: **^{1}H NMR** ($CDCl_3$, 400 MHz, δ ppm): 2.88-3.13 (m, 2H), 3.44 (d, 2H, *J* = 12.8 Hz), 3.73-3.82 (m, 4H), 3.89 (s, 3H, Ar-OCH_3), 3.94 (s, 6H, 2 × Ar-OCH_3), 3.96 (s, 6H, 2 × Ar-OCH_3), 6.02 (s, 2H, -OCH_2O-), 6.12 (s, 2H, -OCH_2O-), 6.65 (s, 2H, 2 × Ar-H), 7.22 (s, 2H, 2 × Ar-H); **^{13}C NMR** ($CDCl_3$, 100 MHz, δ ppm): 36.5, 54.0, 54.7 (2C, 2 × $ArCH_2N$), 56.5 (2C, 2 × OCH_3), 57.0 (2C, 2 × OCH_3), 61.0, 102.2 (2C, 2 × -OCH_2O-), 104.8 (2C, 2 × Ar-C), 110.2 (2C, 2 × Ar-C), 110.5 (2C, 2 × Ar-C), 125.9, 129.4 (2C, 2 × Ar-C), 135.9 (2C, 2 × Ar-C), 140.9, 143.3 (2C, 2 × Ar-C), 146.2 (2C, 2 × Ar-C), 153.2 (2C, 2 × Ar-C), 167.5 (-CONH-); IR (KBr, cm^{-1}): ν 3413, 2357, 1639, 1617, 1585, 1538, 1497, 1434, 1335, 1309, 1232, 1126, 1100, 1050, 923, 856; ESI-MS: m/z: 581.2 $[M+H]^+$.

5.4.12N-(2-(4,10-dimethoxy-6H-[1,3]dioxolo[4',5':3,4]benzo[1,2-c][1,3]dioxolo[4',5':5,6]benzo[1,2-e]azepin-7(8H)-yl)ethyl)-3,4,5-trimethoxybenzamide **(6l)**

The title compound was obtained starting from **5b** and 4-methylbenzoic acid. As a yellow solid, yield: 52.4%; mp: 94.7-96.6 °C. Analytical data for **6l:** ^{1}H NMR ($CDCl_3$, 400 MHz, δ ppm): 2.40 (s, 3H, Ar-CH_3), 2.62-2.73 (m, 1H), 2.86-2.93 (m, 1H), 3.23-3.29 (m, 2H), 3.51-3.58 (m, 2H), 3.62-3.69 (m, 2H), 3.95 (s, 6H, 2 × Ar-OCH_3), 6.00 (d, 2H, -OCH_2O-, *J* = 1.4 Hz), 6.10 (d, 2H, -OCH_2O-, *J* = 1.5 Hz), 6.57 (s, 2H, 2 × Ar-H), 7.23-7.26 (m, 2H, Ar-H), 7.71-7.75 (m, 2H, Ar-H); ^{13}C NMR ($CDCl_3$, 100 MHz, δ ppm): 21.6, 37.2, 53.7, 54.9 (2C, 2 × $ArCH_2N$), 56.8 (2C, 2 × OCH_3), 101.9 (2C, 2 × -OCH_2O-), 109.2 (2C, 2 × Ar-C), 110.6 (2C, 2 × Ar-C), 127.1 (2C, 2 × Ar-C), 128.6 (2C, 2 × Ar-C), 129.3 (2C, 2 × Ar-C), 131.7, 135.1 (2C, 2 × Ar-C), 142.0, 143.0 (2C, 2 × Ar-C), 145.9 (2C, 2 × Ar-C), 167.7 (-CONH-); IR (KBr, cm^{-1}): ν 3413, 2940, 2359, 2341, 1638, 1616, 1489, 1435, 1384, 1305, 1143, 1098, 1049; ESI-MS: m/z: 505.2 $[M+H]^+$.

5.5 Synthesis of ***8a-c***

A solution of Boc-beta-alanine, triethylamine and substituted aniline in DMF was stirried at 0 °C, then HATU was added to the solution. The reaction mixture was stirred at room temperature for 1 h, then diluted with saturated aqueous $NaHCO_3$ and extracted with EtOAc. The organic layer was washed with brine, dried with anhydrous sodium sulfate, filtered and evaporated in vacuo to give corresponding crude compound **7a-c**, respectively. The crude product was purified by column chromatography to yield the title compounds, respectively. And then the Boc-protection group is removed using trifluoroacetic acid (TFA) in dichloromethane to afford compound **8a-c**, which was used in the next without other purification.

*5.6 Synthesis of **9a-c***

Et_3N (0.5 mL, 5eq) was added to the stirred solution of compound **3** (100 mg) and **8a, 8b or 8c** (2eq) in acetonitrile at room temperature under a nitrogen atmosphere. The reaction mixture was stirred and refluxed for 5 h at 60 °C. After the completion of reaction, the mixture was evaporated in vacuo and the residue was diluted with water and extracted with ethyl acetate. The organic layer was washed sequentially with saturated $NaHCO_3$ solution and brine then dried with sodium sulfate, filtered and evaporated in vacuum. The crude product was purified by column chromatography to yield the title compound, respectively

5.6.1.3-(4,10-dimethoxy-6,8-dihydro-7H-[1,3]dioxolo[4',5':3,4]benzo[1,2-c][1,3]dioxolo[4',5':5,6]benzo[1,2-e]azepin-7-yl)-N-(2-methoxyphenyl)propanamide **(9a)**

The title compound was obtained starting from **3** and 3-amino-N-(2-methoxyphenyl) propanamide. As a white solid, yield: 55.1%; mp: 190.2-191.8 °C. Analytical data for **9a:** ^{1}H NMR ($CDCl_3$, 400 MHz, δ ppm): 2.52-3.12 (m, 4H), 3.33 (d, *J* = 11.2 Hz, 2H), 3.61 (m, 5H), 3.94 (s, 6H, 2 × Ar-OCH_3), 6.02 (s, 2H, -OCH_2O-), 6.12 (s, 2H, -OCH_2O-), 6.58 (s, 2H, 2 × Ar-H), 6.81-6.89 (m, 1H, Ar-H), 6.97-7.03 (m, 2H, 2 × Ar-H), 8.38-8.48 (m, 1H, Ar-H), 11.11 (s, 1H,-NH-); ^{13}C NMR ($CDCl_3$, 100 MHz, δ ppm): 34.0, 51.1, 54.6, 55.7 (2C, 2 × ArCH_2N), 56.9 (2C, 2 × OCH_3), 102.0 (2C, 2 × -OCH_2O-), 109.4 (2C, 2 × Ar-C), 110.1 (2C, 2 × Ar-C), 110.6 (2C, 2 × Ar-C), 120.3, 121.1, 123.5, 128.5 (2C, 2 × Ar-C), 135.1 (2C, 2 × Ar-C), 143.0 (2C, 2 × Ar-C), 145.9 (2C, 2 × Ar-C), 148.6, 170.6 (-CONH-); IR (KBr, cm^{-1}): ν 3413, 2926, 2360, 1641, 1602, 1544, 1489, 1431, 1366, 1305, 1237, 1181, 1096, 1044, 918, 832; ESI-MS: m/z: 521.1 $[M+H]^+$.

5.6.2.3-(4,10-dimethoxy-6,8-dihydro-7H-[1,3]dioxolo[4',5':3,4]benzo[1,2-c][1,3]dioxolo[4',5':5,6]benzo[1,2-e]azepin-7-yl)-N-(4-methoxyphenyl)propanamide **(9b)**

The title compound was obtained starting from **3** and3-amino-N-(4-methoxyphenyl) propanamide. As a white solid, yield: 70.8%; mp: 77.6-78.5 °C. Analytical data for **9b:** ^{1}H NMR ($CDCl_3$, 400 MHz, δ ppm): 2.52-2.68 (m, 2H), 2.75-3.05 (m, 2H), 3.30 (d, 2H, *J* = 12.4 Hz), 3.59 (d, 2H, *J* = 8.4 Hz), 3.80 (s, 3H, Ar-OCH_3), 3.95 (s, 6H, 2 × Ar-OCH_3), 6.02 (d, 2H, -OCH_2O-, *J* = 0.8 Hz), 6.12 (d, 2H, -OCH_2O-, *J* = 1.2 Hz), 6.56 (s, 2H, 2 × Ar-H), 6.85 (d, 2H, 2 × Ar-H, *J* = 8.9 Hz), 7.47 (d, 2H, 2 × Ar-H, *J* = 8.9 Hz), 11.07 (s, 1H, -NH-); ^{13}C NMR ($CDCl_3$, 100 MHz, δ ppm): 33.2, 50.6, 54.2 (2C, 2 × ArCH_2N), 55.6, 56.9 (2C, 2 × OCH_3), 102.0 (2C, 2 × -OCH_2O-), 109.1 (2C, 2 × Ar-C), 110.6 (2C, 2 × Ar-C), 114.2 (2C, 2 × Ar-C), 121.1 (2C, 2 × Ar-C), 128.4 (2C, 2 × Ar-C), 132.2, 135.2 (2C, 2 × Ar-C), 143.1 (2C, 2 × Ar-C), 146.0 (2C, 2 × Ar-C), 155.9, 170.3 (-CONH-); IR (KBr, cm^{-1}): ν 3413, 2939, 1639, 1616, 1548, 1511, 1488, 1433, 1304, 1242, 1142, 1097, 1045, 924, 828; ESI-MS: m/z: 521.1 $[M+H]^+$.

5.6.3.3-(4,10-dimethoxy-6,8-dihydro-7H-[1,3]dioxolo[4',5':3,4]benzo[1,2-c][1,3]dioxolo[4',5':5,6]benzo[1,2-e]azepin-7-yl)-N-(3,4-dimethoxyphenyl)propanamide **(9c)**

The title compound was obtained starting from **3** and 3-amino-N-(3,4-dimethoxyphenyl)propanamide. As a white solid, yield: 85.7%; mp: 166.8-168.6 °C. Analytical data for **9c:** ^{1}H NMR ($CDCl_3$, 400 MHz, δ ppm): 2.57-2.72 (m, 2H), 2.79-3.10 (m, 2H), 3.35 (d, 2H, *J* = 12.4 Hz), 3.63 (d, 2H, *J* = 12.8 Hz), 3.87 (s, 3H, Ar-OCH_3), 3.89 (s, 3H, Ar-OCH_3), 3.95 (s, 6H, 2 × Ar-OCH_3), 6.02 (d, 2H, -OCH_2O-, *J* = 1.4 Hz), 6.12 (d, 2H, -OCH_2O-, *J* = 1.4 Hz), 6.59 (d, 2H, 2 × Ar-H, *J* = 2.3 Hz), 6.76-6.81 (m, 1H, Ar-H), 6.85-6.88 (m, 1H, Ar-H), 7.48 (d, 1H, Ar-H, *J* = 2.3 Hz), 11.02 (s, 1H, -NH-); ^{13}C NMR ($CDCl_3$, 100 MHz, δ ppm): 33.3, 50.5, 54.2 (2C, 2 × ArCH_2N), 56.0, 56.2, 57.0 (2C, 2 × OCH_3), 102.0 (2C, 2 × -OCH_2O-), 104.6, 109.5 (2C, 2 × Ar-C), 110.6 (2C, 2 × Ar-C), 111.2, 111.4, 127.9 (2C, 2 × Ar-C), 132.7, 135.4 (2C, 2 × Ar-C), 143.2 (2C, 2 × Ar-C), 145.4, 146.1 (2C, 2 × Ar-C), 149.1, 170.2 (-CONH-); IR (KBr, cm^{-1}): ν 3413, 2939, 2360, 2341, 1637, 1616, 1558, 1514, 1436, 1304, 1214, 1148, 1103, 1053, 924; ESI-MS: m/z: 551.1 $[M+H]^+$.

5.7. Biological assays

5.7.1. Cytotoxicity assay

1×10^4 K562 and K562/A02 cells were seeded in 96-well plates in RPMI-1640 and incubated for 24 h. The exponentially growing cancer cells were incubated with various concentrations of compounds for 72 h at 37 °C (5% CO_2, 95% humidity). After 72 h of incubation, MTS was added directly to the cells. After additional incubation for 3 h at 37 °C, the absorbance at 490 nm was read on a microplate reader (Thermo, USA). The IC_{50} values of the compounds for cytotoxicity were calculated by GraphPad Prism 3.0 software from the dose-response curves.

5.7.2. Flow cytometric analysis

1×10^6 K562/A02 or K562 cells in culture were pre-incubated with different concentrations of the target compounds, VRP or vehicle control (0.1% DMSO) for 1 h at 37 °C, followed by addition of 0.5 μM Rh123 or ADR and incubation for 30 min, respectively. The reaction was stopped by addition of ice-cold PBS and centrifugation, washed with ice-cold PBS three times, and subjected analysis by flow cytometry. The relative values were identified by dividing the fluorescence intensity of each measurement by that of vehicle control.

5.7.3 Wound healing assay

MDA-MB-231 cells were seeded in 6-well plates until confluence. The monolayer of cells was wounded by scraping with a sterile 200 μL pipette tip. After rinsing, each culture twice with PBS to remove detached cells and the addition of compound **6k** or **9c** (5, 15 and 45 μM) in DMEM medium containing 10% FBS, photographs of the wounded area were immediately taken at the time of wounding and thereafter 24 h with an inverted microscope (Olympus) equipped with a digital camera (Nikon, Japan, Tokyo) to determine the relative distance of cell migration.

5.7.4 Chamber migration and invasion assay

In chamber migration assay, transwell system (Corning Costar, Cambridge, MA) was utilized. MDA-MB-231 cells with or without the target compound **6k** or **9c** (5, 15, or 45 μM, 24 h) were suspended in serum-free medium, and then seeded into the upper compartment, while the medium containing 10%

fetal bovine serum was added in the lower compartment. After incubation for 4 h, the non-migrated cells on the upper side of the membrane were removed with a cotton swab. The migrated cells on the bottom surface were fixed with 100% methanol and stained with 0.5% crystal violet. The migrated cells were quantified by manual counting and three randomly chosen fields were analyzed for each group.

Invasion assays were performed with chambers as described previously [34]. The assay was performed essentially as the chamber migration assays above except that transwell chambers were initially coated with matrigel (40 μg/100 μL/chamber) at 37°C for 1 h. After incubation for 24 h, the invaded cells were stained and analyzed as conducted above.

5.7.5 Gelatin zymography assay

Cells were treated with or without isorhamnetin (10, 20, or 40 μM) in serum-free medium for 24 h, and then the supernatants were collected. Gelatin zymography assay was performed according to previous method [34]. After treatment, enzyme-digested regions were observed as white bands against blue background. The zones of enzymatic activity were seen as negatively stained bands.

5.7.6. Western blot analysis

Cells were treated with various concentrations of **6k** or **9c** (5, 15, or 45 μM) for 24 h, then collected and lysed. Western blot analysis was conducted according to previous methods [34]. The membranes were exposed to BCIP/NBT alkaline phosphatase color developing reagent for 15 min. All blots were stripped and reprobed with polyclonal anti-GAPDH to verify equal protein loading.

Acknowledgements

The work was financially supported by National Natural Science Foundation of China (Grant No. 81402789 and 81402969), Natural Science Foundation of Jiangsu Province (Grant No. BK20171179), the Foundation for Jiangsu Six Talent Peaks Program (Grant No. 2017-YY-039) and Jiangsu Provincial 333 High-level Talents Cultivation Project.

References

[1] P. Bugde, R. Biswas, F. Merien, J. Lu, D.X. Liu, M.W. Chen, S.F. Zhou, Y. Li, The therapeutic potential of targeting ABC transporters to combat multi-drug resistance, Expert Opinion on Therapeutic Targets, 21 (2017) 511-530.

[2] S. Shukla, A. Srivastava, S. Kumar, U. Singh, S. Goswami, B. Chawla, M.S. Bajaj, S. Kashyap, J. Kaur, Expression of multidrug resistance proteins in retinoblastoma, International Journal of Ophthalmology, 10 (2017) 1655-1661.

[3] S. Kachalaki, M. Ebrahimi, L.M. Khosroshahi, S. Mohammadinejad, B. Baradaran, Cancer chemoresistance; biochemical and molecular aspects: a brief overview, Eur. J. Pharm. Sci., 89 (2016) 20-30.

[4] J.I. Fletcher, R.T. Williams, M.J. Henderson, M.D. Norris, M. Haber, ABC transporters as mediators of drug resistance and contributors to cancer cell biology, Drug Resist. Update., 26 (2016) 1-9.

[5] T. Hu, Z. Li, C.-Y. Gao, C.H. Cho, Mechanisms of drug resistance in colon cancer and its therapeutic strategies, World J. Gastroentero, 22 (2016) 6876-6889.

[6] W. Li, H. Zhang, Y.G. Assaraf, K. Zhao, X. Xue, J. Xie, D.-H. Yang, Z.-S. Chen, Overcoming ABC transporter-mediated multidrug resistance: Molecular mechanisms and novel therapeutic drug strategies, Drug Resist. Update., 27 (2016) 14-29.

[7] I.L.K. Wong, B.-C. Wang, J. Yuan, L.-X. Duan, Z. Liu, T. Liu, X.-M. Li, X. Hu, X.-Y. Zhang, T. Jiang, S.-B. Wan, L.M.C. Chow, Potent and Nontoxic Chemosensitizer of P-Glycoprotein-Mediated Multidrug Resistance in Cancer: Synthesis and Evaluation of Methylated Epigallocatechin, Gallocatechin, and Dihydromyricetin Derivatives, J. Med. Chem., 58 (2015) 4529-4549.

[8] E. Fox, B.C. Widemann, D. Pastakia, C.C. Chen, S.X. Yang, D. Cole, F.M. Balis, Pharmacokinetic and pharmacodynamic study of tariquidar (XR9576), a P-glycoprotein inhibitor, in combination with doxorubicin, vinorelbine, or docetaxel in children and adolescents with refractory solid tumors, Cancer Chemoth. Pharm., 76 (2015) 1273-1283.

[9] M. Hemmer, S. Krawczyk, I. Simon, A. Hilgeroth, Discovery of substituted 1,4-dihydroquinolines as novel promising class of P-glycoprotein inhibitors: First structure-activity relationships and bioanalytical studies, Bioorg. Med. Chem. Lett, 25 (2015) 3005-3008.

[10] Z. Wang, I.L.K. Wong, F.X. Li, C. Yang, Z. Liu, T. Jiang, T.F. Jiang, L.M.C. Chow, S.B. Wan, Optimization of permethyl ningalin B analogs as P-glycoprotein inhibitors, Bioorg. Med. Chem., 23 (2015) 5566-5573.

[11] A. Palmeira, E. Sousa, M.H. Vasconcelos, M.M. Pinto, Three Decades of P-gp Inhibitors: Skimming Through Several Generations and Scaffolds, Curr. Med. Chem., 19 (2012) 1946-2025.

[12] J. Dinic, A. Podolski-Renic, T. Stankovic, J. Bankovic, M. Pesic, New Approaches With Natural Product Drugs for Overcoming Multidrug Resistance in Cancer, Curr. Pharm. Design., 21 (2015) 5589-5604.

[13] S. Karthikeyan, S.L. Hoti, Development of Fourth Generation ABC Inhibitors from Natural Products: A Novel Approach to Overcome Cancer Multidrug Resistance, Anti-Cancer Agent. Me., 15 (2015) 605-615.

[14] J.B. Chang, Q. Wang, Y.F. Li, Synthesis and biological activity of Wuweizisu C and analogs, Curr. Top. Med. Chem., 9 (2009) 1660-1675.

[15] J. Jin, H. Sun, H. Wei, G. Liu, The anti-hepatitis drug DDB chemosensitizes multidrug resistant cancer cells in vitro and in vivo by inhibiting P-gp and enhancing apoptosis, Invest. New Drug, 25 (2007) 95-105.

[16] X.K. Gu, Z.G. Ren, X.B. Tang, H. Peng, Q. Zhao, Y.S. Lai, S.X. Peng, Y.H. Zhang, Synthesis and biological evaluation of novel bifendate derivatives bearing 6, 7-dihydro-dibenzo[c,e]azepine scaffold as potent P-glycoprotein inhibitors, Eur. J. Med. Chem., 51 (2012) 137-144.

[17] F. Orlandi, M. Coronnello, C. Bellucci, S. Dei, L. Guandalini, D. Manetti, C. Martelli, M.N. Romanelli, S. Scapecchi, M. Salerno, H. Menif, I. Bello, E. Mini, E. Teodori, New structure-activity relationship studies in a series of N,N-bis(cyclohexanol)amine aryl esters as potent reversers of P-glycoprotein-mediated multidrug resistance (MDR), Bioorg. Med. Chem., 21 (2013) 456-465.

[18] S. Dei, M. Coronnello, E. Floriddia, G. Bartolucci, C. Bellucci, L. Guandalini, D. Manetti, M.N. Romanelli, M. Salerno, I. Bello, E. Mini, E. Teodori, Multidrug resistance (MDR) reversers: High activity and efficacy in a series of asymmetrical N,N-bis(alkanol)amine aryl esters, Eur. J. Med. Chem., 87 (2014) 398-412.

[19] E. Teodori, S. Dei, E. Floriddia, M.G. Perrone, D. Manetti, M.N. Romanelli, M. Contino, N.A. Colabufo, Arylamino Esters As P-Glycoprotein Modulators: SAR Studies to Establish Requirements for Potency and Selectivity, Chemmedchem, 10 (2015) 1339-1343.

[20] Y.-H. Wang, M. Goto, L.-T. Wang, K.-Y. Hsieh, S.L. Morris-Natschke, G.-H. Tang, C.-L. Long, K.-H. Lee, Multidrug resistance-selective antiproliferative activity of Piper amide alkaloids and synthetic analogues, Bioorg. Med. Chem. Lett, 24 (2014) 4818-4821.

[21] X.Q. Li, L. Wang, Y. Lei, T. Hu, F.L. Zhang, C.H. Cho, K.K.W. To, Reversal of P-gp and BCRP-mediated MDR by tariquidar derivatives, Eur. J. Med. Chem., 101 (2015) 560-572.

[22] R. Mudududdla, S.K. Guru, A. Wani, S. Sharma, P. Joshi, R.A. Vishwakarma, A. Kumar, S. Bhushan, S.B. Bharate, 3-(Benzo[d][1,3]dioxol-5-ylamino)-N-(4-fluorophenyl)thiophene-2-carboxamide overcomes cancer chemoresistance via inhibition of angiogenesis and P-glycoprotein efflux pump activity, Org. Biomol. Chem., 13 (2015) 4296-4309.

[23] J.E. Hill, M.K. Linder, K.S. Davies, G.A. Sawada, J. Morgan, T.Y. Ohulchanskyy, M.R. Detty, Selenorhodamine Photosensitizers for Photodynamic Therapy of P-Glycoprotein-Expressing Cancer Cells, J. Med. Chem., 57 (2014) 8622-8634.

[24] A. Orchard, G.A. Schamerhorn, B.D. Calitree, G.A. Sawada, T.W. Loo, M.C. Bartlett, D.M. Clarke, M.R. Detty, Thiorhodamines containing amide and thioamide functionality as inhibitors of the ATP-binding cassette drug transporter P-glycoprotein (ABCB1), Bioorg. Med. Chem., 20 (2012) 4290-4302.

[25] R.Z. Pellicani, A. Stefanachi, M. Niso, A. Carotti, F. Leonetti, O. Nicolotti, R. Perrone, F. Berardi, S. Cellamare, N.A. Colabufo, Potent galloyl-based selective modulators targeting multidrug resistance associated protein 1 and P-glycoprotein, J. Med. Chem., 55 (2012) 424-436.

[26] Z. Xu, X. Xu, R. O'Laoi, H. Ma, J. Zheng, S. Chen, L. Luo, Z. Hu, S. He, J. Li, H. Zhang, X. Zhang, Design, synthesis, and evaluation of novel porcupine inhibitors featuring a fused 3-ring system based on the 'reversed' amide scaffold, Bioorg. Med. Chem., 24 (2016) 5861-5872.

[27] Y.G. Ma, M. Wink, Lobeline, a piperidine alkaloid from Lobelia can reverse P-gp dependent multidrug resistance in tumor cells, Phytomedicine., 15 (2008) 754-758.

[28] A. Bisi, S. Gobbi, L. Merolle, G. Farruggia, F. Belluti, A. Rampa, J. Molnar, E. Malucelli, C. Cappadone, Design, synthesis and biological profile of new inhibitors of multidrug resistance associated proteins carrying a polycyclic scaffold, Eur. J. Med. Chem., 92 (2015) 471-480.

[29] J. Jiang, X. Wang, K. Cheng, W. Zhao, Y. Hua, C. Xu, Z. Yang, Psoralen reverses the P-glycoprotein-mediated multidrug resistance in human breast cancer MCF-7/ADR cells, Molecular Medicine Reports, 13 (2016) 4745-4750.

[30] T.N. Trotter, Y. Yang, Matricellular proteins as regulators of cancer metastasis to bone, Matrix Biol., 52-54 (2016) 301-314.

[31] Y.L. Jiang, S.X. Li, Y.J. Liu, L.P. Ge, X.Z. Han, Z.P. Liu, Synthesis and Evaluation of Trehalose-Based Compounds as Novel Inhibitors of Cancer Cell Migration and Invasion, Chemical Biology & Drug Design,

86 (2015) 1017-1029.

[32] Z. Liu, B. Zhang, K. Liu, Z. Ding, X. Hu, Schisandrin B attenuates cancer invasion and metastasis via inhibiting epithelial-mesenchymal transition, PLoS One, 7 (2012) e40480.

[33] H. Sun, G.-T. Liu, Inhibitory effect of dimethyl dicarboxylate biphenyl on invasion of human hepatocellular carcinoma cell line MHCC97-H with high metastasis potential and its mechanisms, Chinese journal of cancer, 25 (2006) 1464-1469.

[34] C.L. Li, D. Yang, Y.W. Zhao, Y. Qiu, X. Cao, Y.Y. Yu, H. Guo, X.K. Gu, X.X. Yin, Inhibitory Effects of Isorhamnetin on the Invasion of Human Breast Carcinoma Cells by Downregulating the Expression and Activity of Matrix Metalloproteinase-2/9, Nutr. Cancer, 67 (2015) 1191-1200.

[35] G. Lobo, M. Monasterios, J. Rodrigues, N. Gamboa, M.V. Capparelli, J. Martinez-Cuevas, M. Lein, K. Jung, C. Abramjuk, J. Charris, Synthesis, crystal structure and effect of indeno[1,2-b]indole derivatives on prostate cancer in vitro. Potential effect against MMP-9, Eur. J. Med. Chem., 96 (2015) 281-295.

Highlights

1. Novel bifendate derivatives were synthesized as anti-MDR and anti-metastasis agents.
2. **6k** and **9c** exhibited high MDR reversal effect by inhibiting P-gp function.
3. **6k** and **9c** markedly suppressed the migration and invasive activity of tumor cells.
4. **6k** and **9c** significantly inhibited MMP-2 and MMP-9 activity and expression in vitro.